

Perpendicular Orientation of Cylindrical Microdomains in Extruded Triblock Copolymer

Kenichi Shimizu,^{*,†} Takeshi Yasuda,[†] and Hiromu Saito[‡]

[†]*Tokyo Metropolitan Industrial Technology Research Institute, Kita-ku, Tokyo 115-8586, Japan, and*

[‡]*Department of Organic and Polymer Materials Chemistry, Tokyo University of Agriculture and Technology, Koganei-shi, Tokyo 184-8588, Japan*

Received July 25, 2009; Revised Manuscript Received December 4, 2009

Introduction

Block copolymers have the ability to self-assemble into various nanostructures, which are often called microdomain structures, depending on the volume fraction, total molecular weight, and interaction parameter.¹ In the self-assembly process, well-ordered nanostructures randomly nucleate and grow to a submicrometer scale and form grain structure similar to a polycrystalline material. The application of external force on block copolymers induces the orientation of the microdomains and a single-crystal-like morphology in which well-ordered nanostructures are extended to a macroscopic scale.^{2,3} The anisotropic properties of the single-crystal-like morphology are expected to be used for many applications such as mechanical,⁴ optical,^{5,6} transport,^{7,8} and so on.⁹ Various shear fields have been examined to acquire macroscopically anisotropic morphology, e.g., extrusion,^{10–14} simple shear,¹⁵ reciprocating shear,^{16–18} press molding,^{19,20} and roll casting.²¹ It has been observed that cylindrical or lamellar microdomains are aligned perpendicular to the shear direction in the vicinity of order–disorder transition^{13,18} and in pentablock copolymer systems.^{14,17} On the other hand, for triblock copolymers with microseparated structures in the melt state, it has been reported that only cylindrical or lamellar microdomains are aligned parallel to the shear direction.^{4–6,10,15,16,21}

Our previous studies²² of small-angle X-ray scattering (SAXS) on polystyrene-*block*-hydrogenated polyisoprene-*block*-polystyrene (SEPS) triblock copolymer revealed that the polystyrene (PS) cylindrical microdomains were aligned parallel to the flow direction and a single-crystal-like morphology was obtained near the shear plane, but they were inclined in the inner region by extrusion through a circular die. With an increase in the shear rate, the region of the single-crystal-like morphology increased by the development of a uniform planar alignment, but PS cylindrical microdomains were randomly aligned at the center of the extruded specimen.

It is well-known that the velocity profile of viscoelastic fluid induced by shear flow varies with the shear rate. When the shear rate is high, a zero-velocity gradient region appears at the center of the shear flow, and this region becomes larger as the shear rate increases. The velocity profile is radially symmetric in the cross section of a circular channel die. In contrast, the velocity profile is anisotropic in the cross section of a rectangular channel die.^{23,24} Because of the anisotropy of the velocity profile in the cross section, characteristic morphologies of the cylindrical microdomains are expected to be obtained by extrusion through a rectangular channel die.

In this study, to understand the relationship between the velocity profile and the morphology of the microdomains in triblock copolymers with microseparated structures in the melt state, we investigated the morphology of PS cylindrical microdomains of SEPS triblock copolymers extruded through a rectangular channel die at different shear rates by SAXS measurement. To clarify the shear-induced orientation of the cylindrical microdomains, SAXS measurements were performed for three different irradiation directions on the extruded specimens. The results are discussed in terms of the velocity profile of the shear flow.

Experimental Section

The SEPS used in this study was a commercial product, SEPTON 2002 (SEPS), manufactured by Kuraray Co., Ltd. SEPS-30 is triblock copolymer with compositions of 30 wt % of PS. The weight-average molecular weight, as determined by size exclusion chromatography, was 5.5×10^4 . The order–disorder transition temperature determined by dynamic mechanical property with oscillatory shear strain of 1% was 275 °C.

The extrusion condition and the die used are shown schematically in Figure 1. Specimens were extruded at plunger speeds of $V = 0.5$ and 500 mm/min through a rectangular die with gap $H = 1$ mm, width $B = 5$ mm, and length $L = 5$ mm at 220 °C using a Capilograph 1C capillary rheometer with barrel radius $R = 9.55$ mm (Toyo Seiki Seisaku-sho, Ltd.). The apparent shear rates at the wall $\dot{\gamma}$ for plunger speeds of $V = 0.5$ and 500 mm/min, calculated by $\dot{\gamma} = 6VR^2/BH^2$, were 0.72 and 720 s^{-1} , respectively.

For SAXS measurement, the extruded rectangular specimens thus obtained were cut into appropriate shapes to obtain a light path length of ca. 1 mm. SAXS was measured on the extruded specimens for three different irradiation directions, as shown in Figure 1. X-rays were irradiated along (i) the flow direction (z -direction), (ii) the velocity gradient direction (y -direction), and (iii) the neutral direction (x -direction). SAXS measurements were performed with a Rigaku RINT 2400 diffractometer (Rigaku Corp.) equipped with a graphite crystal monochromator, a two-pinhole collimator system, and a 2-dimensional imaging plate detector. The monochromatic Cu K α X-ray was generated at 50 kV and 200 mA. Pinhole collimation was obtained with two 0.2 mm pinholes spaced 110 mm apart. X-ray irradiation spots on the specimens were moved at intervals of 0.1 mm using the moving stage with a micrometer. The distance from the sample to the imaging plate was 550 mm.

Results and Discussion

Figure 2 shows the SAXS patterns of SEPS extruded through a rectangular channel die at a shear rate of 0.72 and 720 s^{-1} . Here,

*Corresponding author: Tel +81-3-3909-2151; Fax +81-3-3909-2590; e-mail shimizu.kenichi@iri-tokyo.jp.

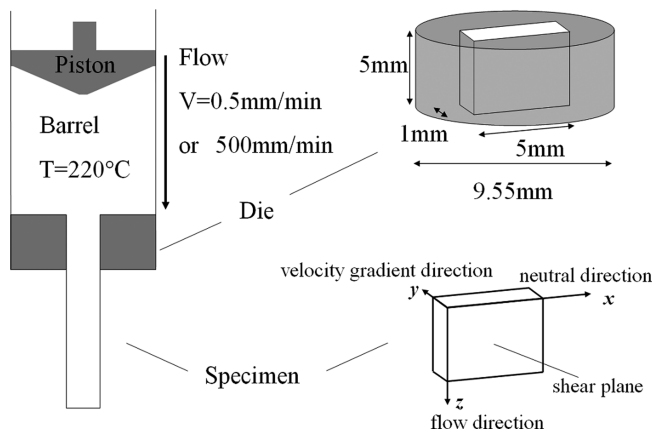


Figure 1. Schematic diagrams of extrusion apparatus and geometry of species for SAXS measurements.

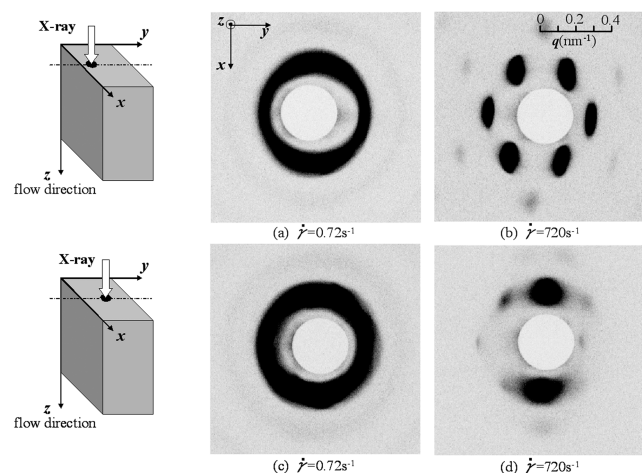


Figure 2. SAXS patterns obtained for SEPS extruded at a shear rate of 0.72 s^{-1} (a, c) and 720 s^{-1} (b, d). X-ray irradiation along the flow direction (z -direction) at the position of 0.2 mm from the edge (a, b) and at the center of the x - y shear plane (c, d). The z -axis is perpendicular to the plane of the paper.

the incident X-ray was irradiated along the flow direction. At the low shear rate of 0.72 s^{-1} , the pattern shows azimuthal intensity distribution due to a pair of peaks along the y -direction and a pair of broad peaks along the x -direction, but it is almost ring at all irradiation spots (Figures 2a and 2c). The results indicate that the (10) cylinder planes are partially aligned parallel to the z - x shear plane, but they are almost randomly oriented and the morphology is not like that of a single crystal (see Figure 5a). In contrast, at the high shear rate of 720 s^{-1} , point patterns are observed and are varied by moving the irradiation spot along the velocity gradient direction (y -direction) from the edge to the center of the cross section (Figures 2b and 2d). Symmetric six-point patterns are observed near the z - x shear plane (Figure 2b). Since a pair of spots is seen along the y -direction in the six-point pattern, such a SAXS pattern indicates a single-crystal-like morphology in which the (10) cylinder planes are parallel to the z - x shear plane and the longitudinal axes of the cylindrical microdomains are aligned parallel to the flow direction near the shear plane, as schematically shown in Figures 5b and 5d. The interesting result here is that a pair of strong diffraction peaks is observed at the center of the cross section (Figure 2d). The pair of strong diffraction peaks indicates that the cylindrical microdomains are aligned perpendicular to the flow direction at the center of the shear flow (see Figure 5b,d).

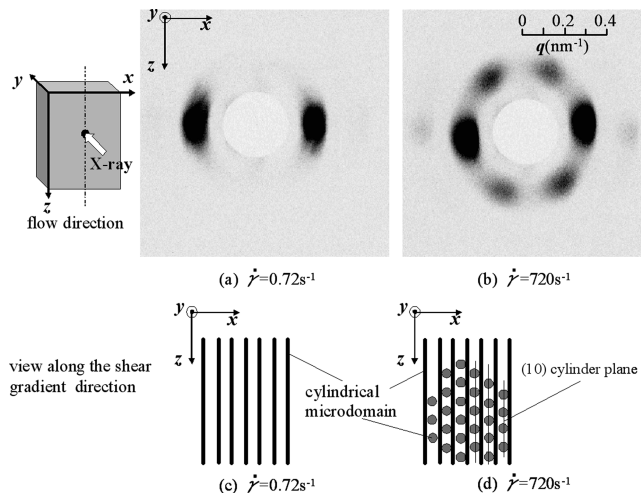


Figure 3. SAXS patterns obtained for SEPS extruded at a shear rate of 0.72 s^{-1} (a) and 720 s^{-1} (b) and schematic diagrams of the PS cylindrical microdomains and the (10) cylinder planes (c, d). The incident X-ray irradiated along the velocity gradient direction (y -direction) at the center of the z - x shear plane. The y -axis is perpendicular to the plane of the paper.

Figures 3a and 3b show SAXS patterns of the as-extruded SEPS measured by the incident X-ray irradiated along the velocity gradient direction (y -direction) at the center of the z - x shear plane. At the low shear rate of 0.72 s^{-1} , a pair of strong diffraction spots is seen along the x -direction (Figure 3a). The results indicate that the longitudinal axes of the cylindrical microdomains are parallel to the flow direction and are not inclined in the neutral direction (x -direction), as schematically shown in Figure 3c. A pair of diffraction spots along the x -direction is also seen in the SEPS extruded at the high shear rate of 720 s^{-1} (Figure 3b). The pair of diffraction spots along the x -direction indicates that the longitudinal axes of the cylindrical microdomains are aligned parallel to the flow direction near the z - x shear plane as demonstrated in Figures 2b and 5b. The interesting result here is that a symmetric six-point pattern, overlapped with the diffraction spots along the x -direction, is observed. The six-point pattern indicates that a single-crystal-like morphology exists at the center of the cross section and the (10) cylinder planes are almost parallel to the y - z plane. This confirms that the well-ordered hexagonally packed cylindrical microdomains are aligned perpendicular to the flow direction and parallel to the velocity gradient direction (y -direction) at the center of the shear flow demonstrated in Figures 2d, 5b, and 5d. In other words, the coexistence of the pair of diffraction peaks and the symmetric six-point pattern shown in Figure 3b indicates that the cylindrical microdomains aligned parallel to the flow direction and those perpendicular to the flow direction are coexisted along the y -direction, as shown in Figure 3d. Thus, the alignment of the microdomains at the center of the flow differs with changes in the shear rate. That is, the longitudinal axes of the single-crystal-like hexagonally packed cylindrical microdomains are aligned perpendicular to the flow direction at the high shear rate while they are not at the low shear rate. The difference in the alignment might be attributed to the difference in the velocity gradient; i.e., the longitudinal axes of the cylindrical microdomains are aligned perpendicular to the flow direction when the velocity gradient is zero at the high shear rate (see Figures 5e and 5f).

Figure 4 shows SAXS patterns of extruded SEPS measured by the incident X-ray irradiated along the neutral direction. A pair of strong diffraction spots is seen along the y -direction near the z - x shear plane at each shear rate (Figures 4a and 4b), indicating that

the longitudinal axes of cylindrical microdomains are parallel to the flow direction near the z - x shear plane. The results of Figures 4a and 4b are consistent with those demonstrated in Figures 3a and 2b, respectively. At the center of the y - z plane, a symmetric pattern with wide azimuthal intensity distribution is seen around the y -direction at the low shear rate (Figure 4c). The peak position in the symmetric pattern is deviated from the y -direction and the angle deviated from the y -direction is about 15° , indicating that the longitudinal axes of the cylindrical microdomains are inclined at an angle of about 15° against the flow direction (see Figure 5c). In contrast, at the high shear rate, a pair

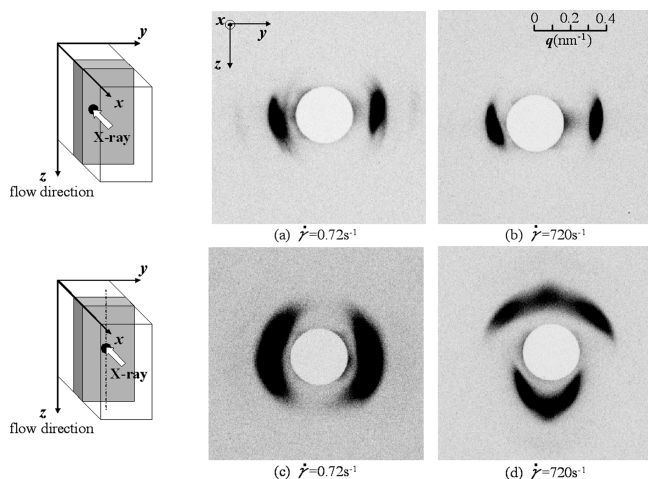


Figure 4. SAXS patterns obtained for SEPS extruded at a shear rate of 0.72 s^{-1} (a, c) and 720 s^{-1} (b, d). X-ray irradiation is along the neutral direction (x -direction) at the position of 0.2 mm from the edge (a, b) and at the center of the y - z shear plane (c, d). The x -axis is perpendicular to the plane of the paper.

of weak diffraction spots along the z -direction and an asymmetric pattern about the y -direction are seen (Figure 4d). The pair of weak diffraction spots along the z -direction indicates that the (10) cylinder planes are almost parallel to the y - z plane and that the longitudinal axes of the short cylindrical microdomains are perpendicular to the flow direction and are parallel to the velocity gradient direction (y -direction), as demonstrated in Figures 2d and 3b. The azimuthal intensity distribution surrounding the z -direction indicates that the longitudinal axes of the cylindrical microdomain in the extruded specimen at the high shear rate are more inclined around the center of the flow than that at the low shear rate (see Figures 5c and 5d). Thus, the alignment of cylindrical microdomains changes along the y -direction. The broad ring pattern shown in Figure 2c and the weak diffraction around the x -direction shown in Figure 2d may be ascribed to the existence of the cylindrical microdomains inclined around the center of the flow. The difference in the alignment around the center of the flow might be attributed to the difference in the velocity profiles along velocity gradient direction (y -direction) at the center of the flow; i.e., the inclination to the flow direction is large when the velocity gradient is small at the high shear rate while it is small when the velocity gradient is large at the low shear rate (see Figures 5e and 5f). The asymmetric pattern shown in Figure 4d is caused by the oblique irradiation of X-ray to the well-ordered (10) cylinder planes. Hence, the asymmetry of the pattern is changed by rotating the specimen and changing X-ray irradiation angle to the cylinder planes.

Since the order-disorder transition temperature is 50°C higher than the extruded temperature and the PS microdomains are elastic in the melt state, the rigid PS cylindrical microdomains would be oriented by the velocity gradient and deposited along the inside surface of shear plane.¹¹ Consequently, the alignment of the cylindrical microdomain is varied with changes in the shear rate. Schematic diagrams of the alignment of the PS cylindrical

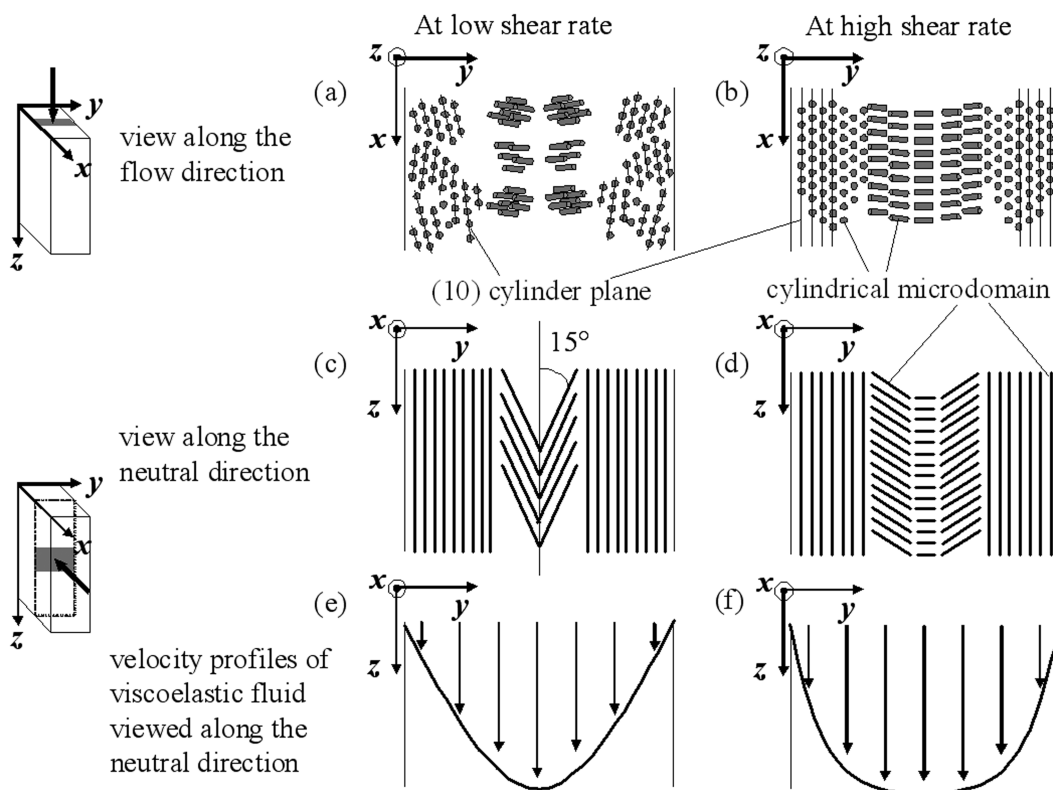


Figure 5. Schematic diagrams of the orientation of PS cylindrical microdomains and the (10) cylinder planes by extrusion through a rectangular die revealed by SAXS measurements (a-d) and the velocity profiles of viscoelastic fluid (e, f).

microdomains of the extrudate suggested from Figures 2–4, and the velocity profiles of viscoelastic fluid are shown in Figure 5. At the low shear rate, the cylindrical microdomains are inclined against the flow direction at the center of the shear flow due to the parabolic velocity profile. In contrast, at the high shear rate, the cylindrical microdomains are aligned perpendicular to the flow direction at the center of the flow due to the equivalent shear strain in which the velocity gradient is zero and the velocity profiles are as flat as plug flow. They are aligned perpendicular to the z - x shear plane because the velocity gradient at the center of the flow is significantly affected by the z - x plane which is closer to the center than the y - z plane.

Conclusions

It was found by extruding SEPS through a rectangular channel die at a high shear rate that single-crystal-like hexagonally packed PS cylindrical microdomains were aligned perpendicular to the flow direction at the center of the shear flow while they were aligned parallel to the flow direction near the shear plane. Such characteristic alignment of the cylindrical microdomains might be attributed to the existence of a zero-velocity gradient region at the high shear rate. In other words, the longitudinal axes of the cylindrical microdomains are perpendicular to the flow direction when the velocity gradient is zero at the center of the flow while they are parallel when a velocity gradient exists near the shear plane.

References and Notes

- (1) Hadjichristidis, N.; Pispas, S.; Floudas, G. *Block Polymers*; John Wiley & Sons, Inc.: Hoboken, NJ, 2003.
- (2) Honeker, C. C.; Thomas, E. L. *Chem. Mater.* **1996**, *8*, 1702–1714.
- (3) Sakurai, S. *Polymer* **2008**, *49*, 2781–2796.
- (4) Odell, J. A.; Keller, A. *Polym. Eng. Sci.* **1977**, *17*, 544–559.
- (5) Folkes, M. J.; Keller, A.; Odell, J. A. *J. Polym. Sci., Part B: Polym. Phys.* **1976**, *14*, 847–859.
- (6) Pixa, R.; Schirrer, R. *Colloid Polym. Sci.* **1981**, *259*, 435–446.
- (7) Kinnig, D. J.; Thomas, E. L.; Ottino, J. M. *Macromolecules* **1987**, *20*, 1129–1133.
- (8) Ehlich, D. E.; Takenaka, M.; Hashimoto, T. *Macromolecules* **1993**, *26*, 492–498.
- (9) Park, M.; Harrison, C.; Chaikin, P. M.; Register, R. A.; Adamson, D. H. *Science* **1997**, *276*, 1401–1404.
- (10) Keller, A.; Pedemonte, E.; Willmouth, F. M. *Nature* **1970**, *225*, 538–539.
- (11) Folks, M. J.; Keller, A.; Scalisi, F. P. *Kolloid Z. Z. Polym.* **251**, 1–4.
- (12) Canevarolo, S. V.; Birley, A. W.; Hemsley, D. A. *Br. Polym. J.* **1986**, *18*, 60–64.
- (13) Leist, H.; Geiger, K.; Wiesner, U. *Macromolecules* **1999**, *32*, 1315–1317.
- (14) Harada, T.; Bates, F. S.; Lodge, T. P. *Macromolecules* **2003**, *36*, 5440–5442.
- (15) Scott, D. B.; Waddon, A. J.; Lin, Y.-G.; Karasz, F. E.; Winter, H. H. *Macromolecules* **1992**, *25*, 4175–4181.
- (16) Hadziioannou, G.; Mathis, A.; Skoulios, A. *Colloid Polym. Sci.* **1979**, *257*, 15–22.
- (17) Vigild, M. E.; Chu, C.; Sugiyama, M.; Chaffin, K. A.; Bates, F. S. *Macromolecules* **2001**, *34*, 951–964.
- (18) Winey, K. I.; Patel, S. S.; Larson, R. G.; Watanabe, H. *Macromolecules* **1993**, *26*, 4373–4375.
- (19) Yamaoka, I.; Kimura, M. *Polymer* **1993**, *34*, 4399–4409.
- (20) Pakura, T.; Saijo, K.; Kawai, H.; Hashimoto, T. *Macromolecules* **1985**, *18*, 1294–1302.
- (21) Albalak, R. J.; Thomas, E. L. *J. Polym. Sci., Part B: Polym. Phys.* **1993**, *31*, 37–46.
- (22) Shimizu, K.; Inomata, K.; Nose, T. *Kobunshi Ronbunshu* **1999**, *56*, 565–570.
- (23) Tadmor, Z.; Gogos, C. G. *Principles of Polymer Processing*; John Wiley & Sons, Inc.: New York, 1979.
- (24) Han, C. D. *Rheology and Processing of Polymeric Materials*; Oxford University Press: New York, 2007; Vol. 2.